Heat and Mass Transfer Research Journal
Vol. 3, No. 1; 2019
Published by CanSRG
http://cansrg.com/journals/hmtrj/

Effects of thermal and molecular diffusion on transient free convection flow along an infinite vertical porous plate

Nepal C. Roy[a], S. Siddiqa[b], Md. A. Hossain[a], Rama Subba Reddy Gorla[c,*]

[a]*Department of Mathematics, University of Dhaka, Dhaka 1000, Bangladesh*
[b]*Department of Mathematics, COMSATS Institute of Information Technology, Attock, Pakistan*
[c]*Department of Mechanical Engineering, Cleveland State University, Cleveland, Ohio 44115 USA*

Abstract

We investigated the effects of thermal and molecular diffusion on transient free convection flow of viscous, incompressible fluid along an infinite vertical porous plate. The governing equations have been reduced to convenient form valid for short, long and all time. The solutions for small and large times have been obtained analytically while the solutions for all time have been carried out numerically using the Keller Box method. A good agreement was found between the numerical solutions for all time and the analytical solutions for short and long time. The astonishing results were that in the case of air, the momentum and concentration boundary layers considerably decrease for higher values of the Schmidt number whereas the maximum velocity increases with the increase of the combined buoyancy parameter. On the contrary, in the case of water, the maximum velocity and the shear stress reduce for higher values of the combined buoyancy parameter. The thicknesses of momentum, thermal and concentration boundary layers are found to decrease owing to the increase of the suction parameter.

1. Introduction

In many physical processes, heat and mass transfer occur simultaneously. For example, due to heating of the earth by sunlight, there arises thermal convection in the atmosphere; however, it might be influenced by the amount of water vapor that is released from the ground into the air. On the other hand, when there exist thermal gradients in a system of water, the heat transfer characteristics can be affected by the presence of species concentration of dissolved materials containing in the water [Numerical Heat Transfer, vol. 2, pp. 233-250, 1979]. These processes occur under buoyancy forces exerted from thermal diffusion and diffusion of chemical species. As a result, in these cases buoyancy forces may be recognized as a contributing factor in the heat and mass transfer. Moreover, this conjugate effect of buoyancy forces could play an important role in many chemical engineering processes where species diffusion occurs owing to the concentration gradients of distinct species.

The combined effects of thermal and mass diffusions in natural convection flow have been investigated by Chen and Yuh [1], Somers [2], Wilcox [3], Gill et al. [4], Gebhart and Pera [5], Pera and Gebhart [6] and many others. All of these studies were confined to steady flows only. Hossain [7] studied the mass transfer effects on the unsteady free convection boundary-layer flow along a vertical flat plate, when the plate temperature oscillates in time about a constant non-zero mean and the species concentration at the plate is constant. An integral method was used to find a solution for zero wall velocity and for a mass transfer velocity at the wall with small–amplitude oscillatory wall temperature. Hossain and Begum [8] investigated analytically the flow past a uniformly accelerated vertical porous and non-porous plate resulting from buoyancy forces that arises from the combination of temperature and

* Corresponding author
Submitted: August 5, 2018 Accepted: December 15, 2018

species concentration for small time regime. Later, effect of mass transfer on the unsteady free convection flow of an electrically conducting and viscous incompressible fluid in the presence of foreign species past a uniformly accelerated vertical porous plate of infinite extent had been investigated by Hossain and Mandal [9].

This paper concerns with the flow of viscous, incompressible fluid near an infinite vertical porous plate in presence of external species. The plate is held fixed and kept at a constant temperature (different from the temperature of the molecules). We further consider that foreign species are present in the fluid that creates differences in species concentration in the fluid. Hence buoyancy force will arise due to density gradients caused by thermal differences and differences in molecules constitution. The viscosity of the fluid is assumed to be constant. Different authors have investigated the present problem, both numerically and analytically, taking horizontal component of velocity as function of time. But the case that of constant normal velocity at the surface has yet not been considered. Here we are addressing this problem.

The governing equations have been solved numerically with a blend of analytical techniques. Iterative finite difference scheme is used to find the solution of equations for all time. Although it was not possible to find the all-time solution analytically, yet we have obtained analytical solutions for small and large time regimes. We then compare between the results obtained from numerical and analytical solutions. An excellent agreement between these solutions has been observed. To measure the relative importance of thermal and molecular diffusion, a parameter ω has been introduced. Its effect on fluid flow has been illustrated. Results obtained for different values of Schmidt number *Sc* and suction parameter, λ, being presented graphically in terms of velocity, temperature and concentration profiles as well as shear-stress, surface heat flux and surface mass flux. In all the above considerations fluid is assumed to be air (Pr = 0.7) and water (Pr = 7.0).

2. Mathematical formalisms

We consider transient free convection flows of viscous, incompressible fluid in the presence of foreign species along a vertical porous plate of infinite extent. The flow of fluid is assumed to be in the direction of $\bar{x}$ -axis which is taken along the plate in the upward direction and the $\bar{y}$ -axis is taken normal to it as in Figure 1.

For $t \leq 0$, the temperature and species concentration at the plate is assumed to be T_∞ and C_∞ respectively. For $t > 0$, temperature of the plate and species concentration on the plate are instantaneously raised to T_w and C_w, and thereafter maintained uniform. We further assume that the transpiration velocity is uniform. The set of equations are written below in terms of fluid velocity $\boldsymbol{V}$, temperature T, concentration of a diffusing species C, gravitational force $\rho\boldsymbol{g}$, and pressure p, μ, K_T and D are the molecular transport properties. As the concentration C of the diffusing species is very small compared to that of the other chemical species present, therefore the concentration equation can be written in the following form.

$$\nabla.\boldsymbol{V} = 0 \tag{1}$$

$$\rho\frac{dV}{d\bar{t}} = \rho\boldsymbol{g} - \nabla p + \mu\nabla^2 V \tag{2}$$

$$\rho C_p\frac{dT}{d\bar{t}} = K_T\nabla^2 T + \beta_T T\frac{Dp}{Dt} + \mu\Phi \tag{3}$$

$$\frac{dC}{d\bar{t}} = D\nabla^2 C \tag{4}$$

where

$$\frac{d}{d\bar{t}}(\ ) = \frac{\partial}{\partial \bar{t}}(\ ) + V.\nabla(\ ) \tag{5}$$

$$V = (\bar{u}, \bar{v}, \bar{w}) \tag{6}$$

$$\nabla = \left(\frac{\partial}{\partial \bar{x}}, \frac{\partial}{\partial \bar{y}}, \frac{\partial}{\partial \bar{z}} \right) \tag{7}$$

$\bar{x}$, $\bar{y}$, $\bar{z}$ are dimensional space variables, $\bar{u}$, $\bar{v}$, $\bar{w}$ are the dimensional component of velocity in $\bar{x}$, $\bar{y}$ and $\bar{z}$ direction, $\bar{t}$ is the dimensional time variable, $\boldsymbol{g}$ = g(1,0,0) is the gravitational force where g is the acceleration due to gravity, T and C are dimensional variables for temperature and concentration in flow field of the fluid. The quantity Φ is the conventional function associated with the thermal effect of the viscous dissipation of energy. In Eq. (3), the pressure term $\beta_T D_p / D\bar{t}$ may be important for gas, for which $\beta = 1/T$. However, in general, for flows of small vertical extent this term may be neglected. We have neglected the Soret-Dufour effect because the thermal-diffusion and the diffusion-thermal effects are of smaller order of magnitude than are the effects described by the Fourier or Fick law.

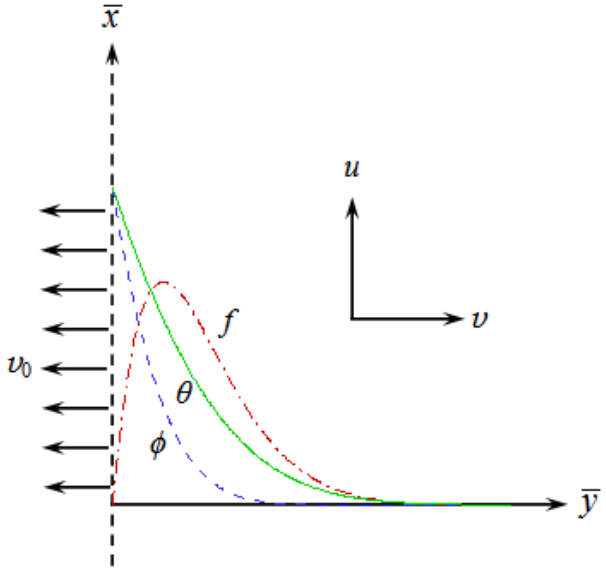

Figure1. Physical configuration and coordinate system.

In Eq. (2), the Boussinesq approximation concerns the combination $\rho\boldsymbol{g} - \nabla p$ in the force-momentum balance. In natural convection flow, we normally disassociate the actual pressure into two components, the local hydrostatic value $p_{\boldsymbol{h}}$ ($\nabla p_{\boldsymbol{h}} = \rho_\infty \boldsymbol{g}$), and the pressure difference in the convection region associated with motion p_m. Consider then the term $\rho\boldsymbol{g} - \nabla p_{\boldsymbol{h}} = \boldsymbol{g}(\rho - \rho_\infty) = g(\rho_\infty - \rho)$, where g is the acceleration due to the gravity, downward in a coordinate system taken positive upward, with reduced density assumed generated over most of the flow region as the net effect of the thermal and mass diffusion. From the series expansion of ρ_∞-ρ in terms of T, p and C, at a given elevation, we come to know that the pressure effect may be neglected and that only the linear term of the temperature effect need be retained for $\beta_T \nabla T << 1$, where $\beta_T = -(1/\rho)(\partial\rho/\partial T)_{P,C}$ is the volumetric coefficient of thermal expansion Gebhart and Pera [5]. A similar argument points that only the linear term of the concentration effect need be retained for $\beta_C \nabla C << 1$, where β_C is the volumetric coefficient of expansion with concentration, that is $\beta_C = -(1/\rho)(\partial\rho/\partial C)_{P,T}$. This latter condition on concentration

differences is met in most atmospheric and oceanic flows. Thus, the term $g(\rho_\infty - \rho)$ is simplified to the following

$$g\left(\rho_\infty - \rho\right) = g\rho\beta_T\left(T - T_\infty\right) + g\rho\beta_C\left(C - C_\infty\right) \tag{8}$$

The second component of the total buoyancy term in (8) is often an important effect in flows of interest.

Now, we consider, for two-dimensional flow, the Prandtl boundary layer approximation that appropriates the situation when the thickness of the flow region (in *y*- direction) is small compared to the distance *x* above the initiation of the natural convection flow. Following Pop and Ingham [10], thus Eqs. (1)-(4) for conservation of mass, momentum, energy, and species concentration can be written as

$$\frac{\partial \bar{u}}{\partial \bar{x}} + \frac{\partial \bar{v}}{\partial \bar{y}} = 0 \tag{9}$$

$$\frac{\partial \bar{u}}{\partial \bar{t}} + \bar{u}\frac{\partial \bar{u}}{\partial \bar{x}} + \bar{v}\frac{\partial \bar{u}}{\partial \bar{y}} = \frac{\partial^2 \bar{u}}{\partial \bar{y}^2} + g\beta_T\left(T - T_\infty\right) + g\beta_C\left(C - C_\infty\right) \tag{10}$$

$$\frac{\partial T}{\partial \bar{t}} + \bar{u}\frac{\partial T}{\partial \bar{x}} + \bar{v}\frac{\partial T}{\partial \bar{y}} = \alpha\frac{\partial^2 T}{\partial \bar{y}^2} \tag{11}$$

$$\frac{\partial C}{\partial \bar{t}} + \bar{u}\frac{\partial C}{\partial \bar{x}} + \bar{v}\frac{\partial C}{\partial \bar{y}} = D\frac{\partial^2 C}{\partial \bar{y}^2} \tag{12}$$

where α and D represent, respectively, the thermal and molecular diffusivity of the fluid. In Eq. (11), the viscous dissipation is neglected being very small in comparison with the conduction terms (Holman [11]). This is a valid assumption, because of small velocities usually encountered in free convection flows.

Before we consider the boundary conditions appropriate for the flow-boundaries, we introduce the following dimensionless variables.

$$\begin{gathered}\bar{u} = \frac{\nu}{L}G_L^{1/2}u, \quad \bar{v} = \frac{\nu}{L}G_L^{1/4}v, \quad \theta = \frac{T - T_\infty}{T_w - T_\infty}, \quad \phi = \frac{C - C_\infty}{C_w - C_\infty}, \quad y = \frac{\bar{y}}{L}G_L^{1/4}, \\ x = \frac{\bar{x}}{L}, \quad \bar{t} = \frac{tL^2}{\nu G_L^{1/2}}, \; G_L = G_T + G_C, \; G_T = \frac{g\beta_T\left(T_w - T_\infty\right)L^3}{\nu^2}, \quad G_C = \frac{g\beta_C\left(C_w - C_\infty\right)L^3}{\nu^2}.\end{gathered} \tag{13}$$

By employing (13) into the set of equations (9)-(12), we get the following set of equations

$$\frac{\partial u}{\partial x} + \frac{\partial v}{\partial y} = 0 \tag{14}$$

$$\frac{\partial u}{\partial t} + u\frac{\partial u}{\partial x} + v\frac{\partial u}{\partial y} = \frac{\partial^2 u}{\partial y^2} + \left(1 - \omega\right)\theta + \omega\phi \tag{15}$$

$$\frac{\partial \theta}{\partial t} + u\frac{\partial \theta}{\partial x} + v\frac{\partial \theta}{\partial y} = \frac{1}{\mathrm{Pr}}\frac{\partial^2 \theta}{\partial y^2} \tag{16}$$

$$\frac{\partial \phi}{\partial t} + u\frac{\partial \phi}{\partial x} + v\frac{\partial \phi}{\partial y} = \frac{1}{Sc}\frac{\partial^2 \phi}{\partial y^2}. \tag{17}$$

Here $\mathrm{Pr} = \nu/\alpha$ is the Prandtl number, $Sc = \nu/D$ is the Schmidt number and $\omega = N/(1+N)$ is the combined buoyancy parameter where $N = G_C/G_T$ measures the relative importance of chemical and thermal diffusion in causing the density difference that drives the flow. It should be mentioned that $N = 0$ corresponds to no species diffusion while $N \to \infty$ to no thermal

diffusion. The parameter ω has been introduced to replace the parameter *N*. The parameter ω is zero and unity according as *N* is zero and infinity.

As the plate is doubly infinite in the vertical direction, this consideration makes the flow unidirectional. Hence all the flow variables will be independent of *x* (see Schilicting [12]). Thus, equations (14)-(17) reduces to

$$\frac{\partial v}{\partial y} = 0 \tag{18}$$

$$\frac{\partial u}{\partial t} + v\frac{\partial u}{\partial y} = \frac{\partial^2 u}{\partial y^2} + (1-\omega)\theta + \omega\phi \tag{19}$$

$$\frac{\partial \theta}{\partial t} + v\frac{\partial \theta}{\partial y} = \frac{1}{\Pr}\frac{\partial^2 \theta}{\partial y^2} \tag{20}$$

$$\frac{\partial \phi}{\partial t} + v\frac{\partial \phi}{\partial y} = \frac{1}{Sc}\frac{\partial^2 \phi}{\partial y^2} \tag{21}$$

The boundary conditions for the flow under consideration can be written as

$$\left.\begin{array}{l} u = 0,\ v = v_0,\ \theta = 1,\ \phi = 1 \ \text{at} \ \ y = 0 \\ u \to 0,\ \theta \to 0,\ \phi \to 0 \ \ \text{as} \ \ y \to \infty \end{array}\right\} \ \text{for all } t > 0 \tag{22}$$

From equation (18), we get straight away that $v = \text{constant or} \, v_0(t)$

It should be mentioned that in all the previous investigations $v_0(t)$ had been assumed to be function of time. This assumption helps in obtaining similarity solution. But here we assume that v is constant; say *s*, which may be termed as transpiration velocity parameter. It should be mentioned that *s* is negative or positive according as fluid is being sucked or blown through the surface of the plate. However, here we assume that $v = s = -\lambda, \ \ \lambda \geq 0.$

Taking the above assumptions into consideration, equations (18)-(21) are re-written as follows.

$$\frac{\partial u}{\partial t} - \lambda\frac{\partial u}{\partial y} = \frac{\partial^2 u}{\partial y^2} + (1-\omega)\theta + \omega\phi \tag{23}$$

$$\frac{\partial \theta}{\partial t} - \lambda\frac{\partial \theta}{\partial y} = \frac{1}{\Pr}\frac{\partial^2 \theta}{\partial y^2} \tag{24}$$

$$\frac{\partial \phi}{\partial t} - \lambda\frac{\partial \phi}{\partial y} = \frac{1}{Sc}\frac{\partial^2 \phi}{\partial y^2} \tag{25}$$

and boundary conditions take the form

$$\left.\begin{array}{l} u = 0, \quad \theta = 1, \quad \phi = 1 \quad \text{at} \ y = 0 \\ u \to 0,\ \theta \to 0,\ \phi \to 0 \ \ \text{as} \ y \to \infty \end{array}\right\} \ \text{for all } t > 0 \tag{26}$$

It is worth mentioning that, the present problem in presence of transverse magnetic field, for an accelerated plate considering v_0 proportional to $t^{-1/2}$, had been investigated by Hossain and Mandal [9] analytically, for small time.

The solution of equation (23)-(26) could be solved using Crank-Nicholson's implicit finite difference method. Instead here we propose to investigate this problem using the similarity concept. To do so, we first reduce these equations to convenient form by introducing the following transformations that are valid for all time regimes

$$u = \frac{t}{t+1} f(\eta, t), \quad \eta = \left(\frac{t}{t+1}\right)^{-1/2} y \tag{27}$$

The boundary layer equations (23)-(26) thus become

$$f'' + \left(\frac{\eta}{2(1+t)^2} + \lambda\left(\frac{t}{t+1}\right)^{1/2}\right) f' - \frac{1}{(1+t)^2} f = \frac{t}{t+1}\frac{\partial f}{\partial t} - (1-\omega)\theta - \omega\phi \tag{28}$$

$$\frac{1}{\mathrm{Pr}}\theta'' + \left(\frac{\eta}{2(1+t)^2} + \lambda\left(\frac{t}{t+1}\right)^{1/2}\right)\theta' = \frac{t}{t+1}\frac{\partial \theta}{\partial t} \tag{29}$$

$$\frac{1}{Sc}\phi'' + \left(\frac{\eta}{2(1+t)^2} + \lambda\left(\frac{t}{t+1}\right)^{1/2}\right)\phi' = \frac{t}{t+1}\frac{\partial \phi}{\partial t} \tag{30}$$

Now we are in a position to integrate the equations (28)-(30) satisfying the following boundary conditions

$$\left.\begin{array}{l} f = 0, \quad \theta = 1, \quad \phi = 1 \quad \text{at } \eta = 0 \\ f \to 0, \ \theta \to 0, \ \phi \to 0 \quad \text{as } \eta \to \infty \end{array}\right\} \ \text{for all } t > 0 \tag{31}$$

In section 3, we will find solutions of equations (28)-(31) for all time using the implicit finite difference method. In the same section, solutions are also obtained for small and large times by the use of perturbation technique.

Having obtained the values of *f*, θ, and ϕ we can easily determine the shear stress $\overline{\tau}$, rate of heat transfer $\overline{q}$, and rate of mass transfer $\overline{m}$, that are calculated from the following relations

$$\overline{\tau} = \mu\left(\frac{\partial \overline{u}}{\partial \overline{y}}\right)_{\overline{y}=0} \tag{32}$$

$$\overline{q} = -K_T\left(\frac{\partial T}{\partial \overline{y}}\right)_{\overline{y}=0} \tag{33}$$

$$\overline{m} = -K_C\left(\frac{\partial C}{\partial \overline{y}}\right)_{\overline{y}=0} \tag{34}$$

where K_T and K_C represent thermal conductivity and coefficient of diffusion. In terms of dimensionless parameters (13) and transformation defined in (27), quantities in (32)-(34) can be rewritten as

$$\tau = \left(\frac{t}{1+t}\right)^{1/2} f'(0) \tag{35}$$

$$q = -\left(\frac{t}{1+t}\right)^{-1/2} \theta'(0) \tag{36}$$

$$m = -\left(\frac{t}{1+t}\right)^{-1/2} \phi'(0) \tag{37}$$

where τ, q and m, are respectively the dimensionless shear-stress, rate of heat-transfer, and the rate of mass-transfer, as defined below

$$\tau = \frac{\overline{\tau} G_L^{-3/4}}{\mu^2/\rho L^2}, \quad q = \frac{\overline{q} G_L^{-1/4}}{K_T(T_w - T_\infty)/yL}, \quad m = \frac{\overline{m} G_L^{-1/4}}{K_C(C_w - C_\infty)/yL} \tag{38}$$

Once we know the values of $f'(0)$, $\theta'(0)$, and $\phi'(0)$ we are at a position to discuss the effects of different physical parameters such as the suction parameter λ, the buoyancy parameter ω and

Schmidt number *Sc* on the shear-stress, rate of heat transfer and the rate of mass transfer, for fluid to be air (Pr = 0.7) or water (Pr = 7.0) in presence of different species.

3. Methods of Solution

The solution of the problem has been obtained using numerical and analytical techniques. We calculated the all time solution employing finite difference together with the Keller Box elimination scheme; whereas, asymptotic solutions for small and large time regimes are obtained analytically.

3.1 All time solution

The solution of the equations (28)-(31) valid for all time has been approximated numerically. We have coupled system of linear differential equations with variable coefficients. We have used iterative implicit finite difference method together with Keller Box elimination scheme to integrate the equations. It's a good approach, since the equations are coupled for non-zero value of ω. To apply the numerical method, we first need to convert the equations (28)–(31) into a system of first order equations as

$$\frac{\partial f}{\partial \eta} = U, \quad \frac{\partial \theta}{\partial \eta} = p, \quad \frac{\partial \phi}{\partial \eta} = q \tag{39}$$

$$U' + p_1 U - p_2 f = p_3 \frac{\partial f}{\partial t} - (1-\omega)\theta - \omega\phi \tag{40}$$

$$\frac{1}{\mathrm{Pr}} p' + p_1 p = p_3 \frac{\partial \theta}{\partial t} \tag{41}$$

$$\frac{1}{Sc} q' + p_1 q = p_3 \frac{\partial \phi}{\partial t} \tag{42}$$

$$\begin{aligned} f(0,t) &= 0, \quad \theta(0,t) = 1, \quad \phi(0,t) = 1 \\ f(\infty,t) &= 0, \quad \theta(\infty,t) = 0, \quad \phi(\infty,t) = 0 \end{aligned} \tag{43}$$

where the values of constants involved in (40)-(42) are given as

$$p_1 = \frac{\eta}{2(1+t^2)} + \lambda \frac{t}{1+t}, \quad p_2 = \frac{1}{(1+t)^2}, \quad p_3 = \frac{t}{1+t} \tag{44}$$

The points in net rectangle, considered on (t,η) plane, are of following structure

$$\begin{aligned} t^0 &= 0, \quad t^m = t^{m-1} + k_m, \quad m = 1,2,3,\cdots\cdots \\ \eta_0 &= 0, \quad \eta_j = \eta_{j-1} + l_j, \quad j = 1,2,3,\cdots\cdots \end{aligned} \tag{45}$$

where m and j are indexes of the sequence of points on (t,η) plane, l_j and k_m are the variable mesh widths. The quantities $(f, U, \theta, p, \phi, q)$ at the net points of the net are approximated by net functions, denoted by $\left(f_j^m, U_j^m, \theta_j^m, p_j^m, \phi_j^m, q_j^m\right)$. We will assume that $f_j^m, U_j^m, \theta_j^m, p_j^m, \phi_j^m, q_j^m$ are known for $0 \le j \le J$, this gives us a system of $6J+6$ linear algebraic equations with $6J+6$ unknowns. The resulting coefficient matrix is tridiagonal that is solved using well-known Thomas algorithm. This whole procedure of reduction to first order form followed central difference approximations and block Thomas algorithm is known as Keller Box method [13].

Initially (t = 0.0), we have to prescribe the guess profile for the functions f, θ, ϕ and their derivatives. These profiles are then incorporated to the Keller Box scheme to march step by step in time t values.

3.2 Solution for small time t

If we assume time *t* to be small then some terms in (28)-(31) can be neglected. The resulting system of equations then becomes

$$f''+\left(\frac{\eta}{2}+\lambda\sqrt{t}\right)f'-f=t\frac{\partial f}{\partial t}-(1-\omega)\theta-\omega\phi \tag{46}$$

$$f(0)=f(\infty)=0$$

$$\frac{1}{\Pr}\theta''+\left(\frac{\eta}{2}+\lambda\sqrt{t}\right)\theta'=t\frac{\partial\theta}{\partial t} \tag{47}$$

$$\theta(0)=1,\ \theta(\infty)=0$$

$$\frac{1}{Sc}\phi''+\left(\frac{\eta}{2}+\lambda\sqrt{t}\right)\phi'=t\frac{\partial\phi}{\partial t} \tag{48}$$

$$\phi(0)=1,\ \phi(\infty)=0$$

The solutions of (46)-(48), found analytically, are given by

$$\theta=\frac{erfc\left\{\sqrt{\Pr}\left(\frac{\eta}{2}+\lambda\sqrt{t}\right)\right\}}{erfc\left(\lambda\sqrt{\Pr t}\right)} \tag{49}$$

$$\phi=\frac{erfc\left\{\sqrt{Sc}\left(\frac{\eta}{2}+\lambda\sqrt{t}\right)\right\}}{erfc\left(\lambda\sqrt{Sc\,t}\right)} \tag{50}$$

$$-f=\sqrt{\frac{2}{\pi}}\frac{1-\omega}{(\Pr-1)erfc\left(\lambda\sqrt{\Pr t}\right)}\frac{G_1(P_1-P_2)}{G_2}+\sqrt{\frac{2}{\pi}}\frac{\omega}{(Sc-1)erfc\left(\lambda\sqrt{Sct}\right)}\frac{G_1(P_1-P_3)}{G_2} \tag{51}$$

where

$$G_1=\sqrt{\frac{\pi}{2}}\left(1+2\lambda^2\Pr t\right)erfc\left(\lambda\sqrt{\Pr t}\right)-\lambda\sqrt{2\Pr te}^{-\lambda^2\Pr t}$$

$$G_2=\sqrt{\frac{\pi}{2}}\left(1+2\lambda^2 t\right)erfc\left(\lambda\sqrt{t}\right)-\lambda\sqrt{2te^{-\lambda^2 t}}$$

$$G_3=\sqrt{\frac{\pi}{2}}\left(1+2\lambda^2 Sct\right)erfc\left(\lambda\sqrt{Sct}\right)-\lambda\sqrt{2Sc\,te}^{-\lambda^2 Sct}$$

$$P_1=\sqrt{\frac{\pi}{2}}\left\{1+2\left(\frac{\eta}{2}+\lambda\sqrt{t}\right)^2\right\}erfc\left(\frac{\eta}{2}+\lambda\sqrt{t}\right)-\sqrt{2}\left(\frac{\eta}{2}+\lambda\sqrt{t}\right)e^{-\left(\frac{\eta}{2}+\lambda\sqrt{t}\right)^2}$$

$$P_2=\sqrt{\frac{\pi}{2}}\left\{1+2\Pr\left(\frac{\eta}{2}+\lambda\sqrt{t}\right)^2\right\}erfc\left\{\sqrt{\Pr}\left(\frac{\eta}{2}+\lambda\sqrt{t}\right)\right\}-\sqrt{2\Pr}\left(\frac{\eta}{2}+\lambda\sqrt{t}\right)e^{-\Pr\left(\frac{\eta}{2}+\lambda\sqrt{t}\right)^2}$$

$$P_3=\sqrt{\frac{\pi}{2}}\left\{1+2Sc\left(\frac{\eta}{2}+\lambda\sqrt{t}\right)^2\right\}erfc\left\{\sqrt{Sc}\left(\frac{\eta}{2}+\lambda\sqrt{t}\right)\right\}-\sqrt{2Sc}\left(\frac{\eta}{2}+\lambda\sqrt{t}\right)e^{-Sc\left(\frac{\eta}{2}+\lambda\sqrt{t}\right)^2}.$$

With a view to determining the values of wall shear stresses, rate of heat and mass transfer for small time, we need to find the values of $\theta'(0,t),\phi'(0,t),\ f'(0,t)$ which are given below.

$$-\theta'(0,t)=\frac{1}{Erfc\left(\lambda\sqrt{\Pr t}\right)}\sqrt{\frac{\Pr}{\pi}}e^{-\Pr\lambda^2 t} \tag{52}$$

$$-\phi'(0,t)=\frac{1}{Erfc\left(\lambda\sqrt{Sct}\right)}\sqrt{\frac{Sc}{\pi}}e^{-Sc\lambda^2 t} \tag{53}$$

$$\begin{aligned} f'(0,t)=&\frac{1-w}{\Pr-1}\frac{G_1}{G_2}\left\{-\lambda\Pr\sqrt{\pi t}erfc\left(\lambda\sqrt{\Pr t}\right)+\sqrt{\Pr}e^{-\lambda^2\Pr t}+\lambda\sqrt{\pi t}erfc\left(\lambda\sqrt{t}\right)-e^{-\lambda^2 t}\right\}\\ &+\frac{w}{Sc-1}\frac{G_1}{G_2}\left\{-\lambda Sc\sqrt{\pi t}erfc\left(\lambda\sqrt{Sct}\right)+\sqrt{Sc}e^{-\lambda^2 Sct}+\lambda\sqrt{\pi t}erfc\left(\lambda\sqrt{t}\right)-e^{-\lambda^2 t}\right\}\end{aligned} \tag{54}$$

The calculated results (52)-(54) are valid for small times only. In section 4, we have made comparison of these results with our numerical solutions uniformly valid for all times. The comparison is given in the form of table, for air (Pr = 0.70) in presence of Hydrogen (*Sc* = 0.22) whilst λ = 0.5, 1.0, 1.5 and ω = 0.5.

3.3 Solution for large time t

The equations governing the flow for large time regime can be obtained from (28)-(31) by considering time *t* to be large. This allows us to neglect few terms that reduces the equations to the following form.

$$f''+\left(\frac{\eta}{2t^2}+\lambda\right)f'-\frac{1}{t^2}f=\frac{\partial f}{\partial t}-(1-\omega)\theta-\omega\phi \tag{55}$$

$$f(0)=f(\infty)=0$$

$$\frac{1}{\Pr}\theta''+\left(\frac{\eta}{2t^2}+\lambda\right)\theta'=\frac{\partial\theta}{\partial t} \tag{56}$$

$$\theta(0)=1,\ \theta(\infty)=0$$

$$\frac{1}{Sc}\phi''+\left(\frac{\eta}{2t^2}+\lambda\right)\phi'=\frac{\partial\phi}{\partial t} \tag{57}$$

$$\phi(0)=1,\ \phi(\infty)=0$$

As we are considering large values of time, so the term $1/t^2$ can be regarded as small parameter. The straight forward expansion of f, θ, and ϕ, in power of t^{-2}, can be written as

$$f=\sum_{i=0}^{n}t^{-2i}f_i,\quad \theta=\sum_{i=0}^{n}t^{-2i}\theta_i,\quad \phi=\sum_{i=0}^{n}t^{-2i}\phi_i \tag{58}$$

We are taking into account just three terms of the expansion (n=2), because higher order terms will not be making significant contributions. Using the Eq. (58) in (55)-(57) and equating the terms of t^{-2i} (i = 0,1,2), we get corresponding zeroth, first and second order problem.

$O(t^0)$:

$$\begin{aligned} &f_0''+\lambda f_0'+(1-\omega)\theta_0-\omega\phi_0=0;\ \ f_0(0)=f_0(\infty)=0\\ &\frac{1}{\Pr}\theta_0''+\lambda\theta_0'=0;\ \ \theta_0(0)=1,\ \theta_0(\infty)=0\\ &\frac{1}{Sc}\phi_0''+\lambda\phi_0'=0;\ \ \phi_0(0)=1,\ \ \phi_0(\infty)=0\end{aligned} \tag{59}$$

$O(t^{-2})$:

$$f_1''+\frac{\eta}{2}f_0'-f_0+\lambda f_1'+(1-\omega)\theta_1-\omega\phi_1=0;\;\; f_1(0)=f_1(\infty)=0$$
$$\frac{1}{\Pr}\theta_1''+\lambda\theta_1'+\frac{\eta}{2}\theta_0'=0;\quad \theta_1(0)=1,\;\theta_1(\infty)=0 \tag{60}$$
$$\frac{1}{Sc}\phi_1''+\lambda\phi_1'+\frac{\eta}{2}\phi_0'=0;\quad \phi_1(0)=1,\;\phi_1(\infty)=0$$

$O(t^{-4})$:

$$f_2''+\frac{\eta}{2}f_1'+\lambda f_2'+(1-\omega)\theta_2-\omega\phi_2=0;\;\; f_2(0)=f_2(\infty)=0$$
$$\frac{1}{\Pr}\theta_2''+\lambda\theta_2'+\frac{\eta}{2}\theta_{02}'+\theta_1=0;\quad \theta_2(0)=1,\;\theta_2(\infty)=0 \tag{61}$$
$$\frac{1}{Sc}\phi_2''+\lambda\phi_2'+\frac{\eta}{2}\phi_1'+\phi_1=0;\quad \phi_2(0)=1,\;\phi_2(\infty)=0$$

One can see that equations (59)-(61) are linear, ordinary differential equations of second order. Solutions of the above equations, found analytically, are given below.

$$\theta_0=e^{-\lambda\Pr\eta},\;\phi_0=e^{-\lambda Sc\eta} \tag{62}$$

$$f_0=\left(\frac{1-\omega}{\lambda^2\Pr(\Pr-1)}+\frac{\omega}{\lambda^2 Sc(Sc-1)}\right)e^{-\lambda\eta}-\frac{1-\omega}{\lambda^2\Pr(\Pr-1)}e^{-\lambda\Pr\eta}-\frac{\omega}{\lambda^2 Sc(Sc-1)}e^{-\lambda Sc\eta} \tag{63}$$

$$\theta_1=-\frac{\Pr}{2}\left(\frac{\eta}{\lambda\Pr}+\frac{\eta^2}{2}\right)e^{-\lambda\Pr\eta},\quad \phi_1=-\frac{Sc}{2}\left(\frac{\eta}{\lambda Sc}+\frac{\eta^2}{2}\right)e^{-\lambda Sc\eta} \tag{64}$$

$$f_1=\left(C_1^0-C_1^1\eta-C_1^2\eta^2\right)e^{-\lambda\eta}-\left(C_1^3+C_1^4\eta+C_1^5\eta^2\right)e^{-\lambda\Pr\eta}-\left(C_1^6+C_1^7\eta+C_1^7\eta^2\right)e^{-\lambda Sc\eta} \tag{65}$$

$$\theta_2=-\left(\frac{1}{\lambda^3\Pr}\eta+\frac{1}{4\lambda^2}\eta^2-\frac{\Pr}{24\lambda}\eta^3-\frac{\Pr^2}{32\lambda}\eta^4\right)e^{-\lambda\Pr\eta} \tag{66}$$

$$\phi_2=-\left(\frac{1}{\lambda^3 Sc}\eta+\frac{1}{4\lambda^2}\eta^2-\frac{Sc}{24\lambda}\eta^3-\frac{Sc^2}{32\lambda}\eta^4\right)e^{-\lambda Sc\eta} \tag{67}$$

$$\begin{aligned}f_2=&\left(C_2^0+C_2^1\eta+C_2^2\eta^2+C_2^3\eta^3+C_2^4\eta^4\right)e^{-\lambda\eta}\\&-\left(C_2^5+C_2^6\eta+C_2^7\eta^2+C_2^8\eta^3+C_2^9\eta^4\right)e^{-\lambda\Pr\eta}\\&-\left(C_2^{10}+C_2^{11}\eta+C_2^{12}\eta^2+C_2^{13}\eta^3+C_2^{14}\eta^4\right)e^{-\lambda Sc\eta}\end{aligned} \tag{68}$$

Using the Eq. (58), the final expressions for $f'(0,t),\theta'(0,t),\phi'(0,t),$ that we have formulated by considering first three terms of the expansion is

$$\theta'(0,t)=-\left(\theta_0'(0)+\frac{1}{t^2}\theta_1'(0)+\frac{1}{t^4}\theta_2'(0)\right) \tag{69}$$

$$\phi'(0,t)=-\left(\phi_0'(0)+\frac{1}{t^2}\phi_1'(0)+\frac{1}{t^4}\phi_2'(0)\right) \tag{70}$$

$$f'(0,t)=-\left(f_0'(0)+\frac{1}{t^2}f_1'(0)+\frac{1}{t^4}f_2'(0)\right) \tag{71}$$

where $\theta_i'(0),\phi_i'(0),f_i'(0)$, i = 0,1,2 are given by

$$\theta_0'(0)=-\lambda\Pr,\;\; \theta_1'(0)=-\frac{1}{2\lambda},\;\; \theta_2'(0)=-\frac{1}{\lambda^3\Pr} \tag{72}$$

$$\phi_0'(0) = -\lambda Sc,\ \ \phi_1'(0) = -\frac{1}{2\lambda},\ \phi_2'(0) = -\frac{1}{\lambda^3 Sc} \tag{73}$$

$$f_0'(0) = \frac{1-\omega}{\lambda \Pr} + \frac{\omega}{\lambda Sc} \tag{74}$$

$$f_1'(0) = -\lambda C_1^0 - C_1^1 + \lambda \Pr C_1^3 - C_1^4 + \lambda Sc C_1^6 - C_1^7 \tag{75}$$

$$f_2'(0) = -\lambda C_2^0 - C_2^1 + \lambda \Pr C_2^5 - C_2^6 + \lambda Sc C_2^{10} - C_2^{11} \tag{76}$$

Analytical solutions thus obtained for large values of time *t* in terms of shear-stress, heat and mass transfer coefficients, for air (i.e., Pr = 0.7) in presence of H_2 (i.e., *Sc* = 0.22), taking different values of suction parameter λ, are entered in Table 1 and are compared with that obtained by the finite difference solutions for all time model.

4. Results and Discussions

All through the numerical calculations the fluid is assumed to be air or water. The values of Pr for air and water at 20^oC and 1atm pressure are given to be 0.7 and 7.0, respectively (see Gebhart and Pera [5]). The values of *Sc* are chosen in a way that they represent the diffusing chemical species of most common interest in air and water Gebhart and Pera [5], such as H_2, He, H_2O, NH_3, and CO_2. For example, in air at 25^oC due to presence of H_2, CO_2, H_2O and NH_3, value of Schmidt number *Sc* is 0.22, 0.30, 0.60, 0.78 and 0.94 respectively. In water, value of *Sc* due to presence of H_2, CO_2 and NH_3 is 152, 453, 445 respectively.

4.1 For air (Pr = 0.7)

In this section we will discuss the results for air (i.e. Pr = 0.7). In order to validate the numerical solutions, a comparison of all time numerical results with the analytical solutions for small and large time are tabulated in Table 1 in terms of wall shear stress, heat and mass transfers. The table shows the analytical and numerical values of shear stress, heat transfer and mass transfer in air in the presence of Hydrogen. It is seen that the numerical results are in good agreement with those obtained by the analytical solutions. The relative error in the numerical and analytical results is even less than 0.5%. This observation serves as strong argument in support of the present numerical results.

Table 1. Comparison of numerical and analytical results for the coefficients of heat and mass transfers and shear stress for different values of suction parameter λ while Pr =0.70, *Sc* =0.22, ω =0.5.

λ	*t*	$(\partial\theta/\partial y)_{y=0}$		$(\partial\phi/\partial y)_{y=0}$		$(\partial u/\partial y)_{y=0}$	
		Numerical	Analytical	Numerical	Analytical	Numerical	Analytical
0.5	0.01	4.94530	4.94536	2.72169	2.71699	0.06997	0.06938
	0.03	2.91481	2.95175	1.59083	1.59843	0.12147	0.12047
	0.05	2.29934	2.33831	1.24409	1.25411	0.15730	0.15578
	0.07	1.97076	2.01202	1.05976	1.07086	0.18666	0.18458
	⋮	⋮	⋮	⋮	⋮	⋮	⋮
	200.0	0.35002	0.35001	0.11017	0.11001	5.91191	5.96834
	220.0	0.35002	0.35001	0.11012	0.11001	5.92963	5.96937
	240.0	0.35002	0.35000	0.11010	0.11000	5.93998	5.97006
	300.0	0.35002	0.3500	0.11006	0.11000	5.95631	5.97157
1.0	0.01	5.16113	5.17478	2.7887	2.78789	0.07092	0.06960
	0.03	3.11146	3.18580	1.65010	1.67047	0.12331	0.12106
	0.05	2.49168	2.57545	1.30268	1.32673	0.16007	0.15669
	0.07	2.16429	2.25162	1.11837	1.14393	0.19305	0.18754
	⋮	⋮	⋮	⋮	⋮	⋮	⋮
	48.0	0.7005	0.70021	0.22063	0.22022	2.95829	2.97485

	50.0	0.7005	0.70021	0.22031	0.22020	2.95740	2.97579
	60.0	0.7005	0.70014	0.22015	0.22014	2.97233	2.97918
	70.0	0.7005	0.70010	0.22008	0.22010	2.97989	2.98132
1.5	0.01	5.38020	5.40844	2.85662	2.85986	0.07186	0.06981
	0.03	3.31136	3.42684	1.71058	1.74381	0.12505	0.12153
	0.05	2.69302	2.82130	1.36286	1.40098	0.16264	0.15732
	0.07	2.36851	2.50122	1.17887	1.21891	0.19373	0.18646
	⋮	⋮	⋮	⋮	⋮	⋮	⋮
	18.0	1.05008	1.05229	0.33100	0.33229	1.95180	1.96583
	20.0	1.05008	1.05187	0.33071	0.33188	1.96248	1.97044
	25.0	1.05007	1.05121	0.33031	0.33121	1.97832	1.97786
	30.0	1.05007	1.05081	0.33014	0.33081	1.98589	1.98230

In Figure 2(a)-(b), we have presented numerical and analytical results in terms of shear stress and mass transfer coefficients for air in presence of H_2 (Sc = 0.22) while λ = 1.0 and ω = 0.5. It is found from the figure that the numerical and analytical solutions are in excellent agreement for all values of Schmidt number Sc. On the other hand, we observe from Figure 2(a) that when the value of Sc is increased the values of shear stress decrease. It is because increasing Sc means that the diffusion coefficient of the fluid is decreased. Therefore, the molecules will conduct less amount of mass, hence concentration at a point will decrease. As a result, velocities will decrease. However, the rate of mass transfer coefficient increases with increasing values of Schmidt number, Sc. It is because the larger value of Sc means a decrease in diffusion coefficient and as a result concentration at a point will be lower for higher Sc. Consequently, there is an increase in the rate of mass transfer coefficient with an increase of Sc.

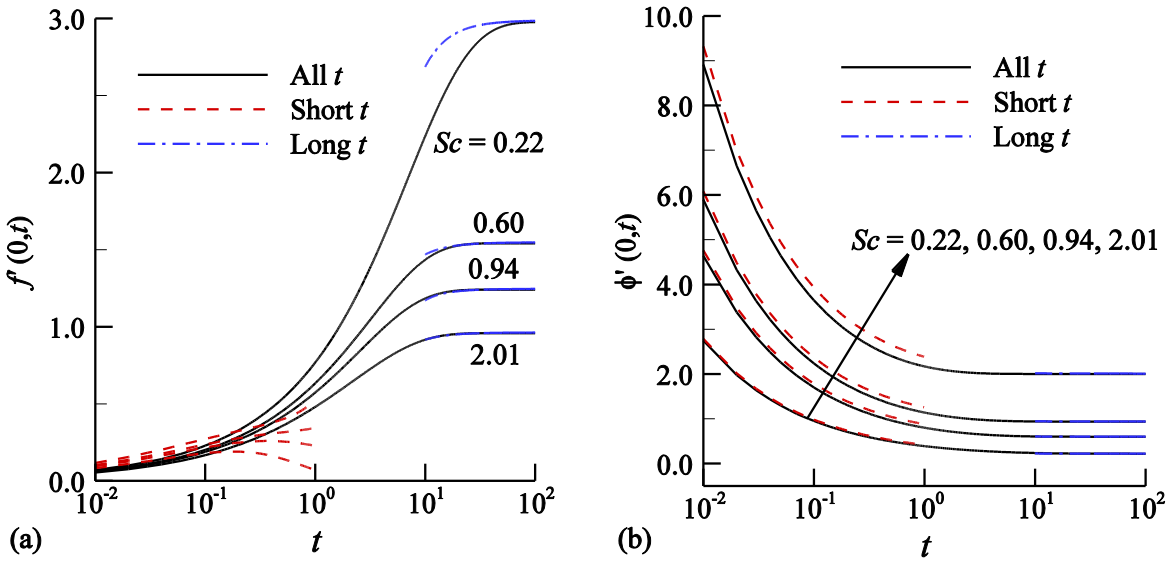

Figure 2. Comparison of (a) shear stress coefficient and (b) mass transfer coefficient against t for different values of Sc while Pr =0.70, λ =1.0, ω =0.5.

4.1 For air (Pr = 0.7)

In this section we will discuss the results for air (i.e. Pr = 0.7). In order to validate the numerical solutions, a comparison of all time numerical results with the analytical solutions for small and large time are tabulated in Table 1 in terms of wall shear stress, heat and mass transfers. The table shows the analytical and numerical values of shear stress, heat transfer and mass transfer in air in the presence of Hydrogen. It is seen that the numerical results are

in good agreement with those obtained by the analytical solutions. The relative error in the numerical and analytical results is even less than 0.5%. This observation serves as strong argument in support of the present numerical results.

The variations of the velocity and concentration profiles for different values of *Sc* are demonstrated in Figure 3(a)-(b). Results show that the momentum and concentration boundary layer thicknesses significantly decrease owing to the increase of *Sc*. The Schmidt number *Sc* (= *v*/*D*) is defined as the ratio of kinematic viscosity to the mass diffusivity. From physical point of view, either the kinematic viscosity is high or the mass diffusivity is low for the larger values of *Sc*. Accordingly, the momentum and concentration boundary layer thicknesses are found to decrease for higher values of *Sc*.

Figure 4 illustrates the numerical results for velocity profiles of fluid particles for different values of the combined buoyancy parameter ω at t = 1.0. The parameter ω acts as controlling parameter between thermal and molecular diffusion. It measures the relative importance of thermal and molecular diffusion in causing buoyancy effects. The value of combined buoyancy parameter ω is 0 for no species diffusion and 1 for no thermal diffusion. The intermediate values of ω gives the combined buoyancy effect due to thermal as well as molecular diffusion. It is evident from the figure that the maximum velocity increases due to the increase of ω. The reason for such a characteristic is that the species diffusion is higher for increasing values of ω.

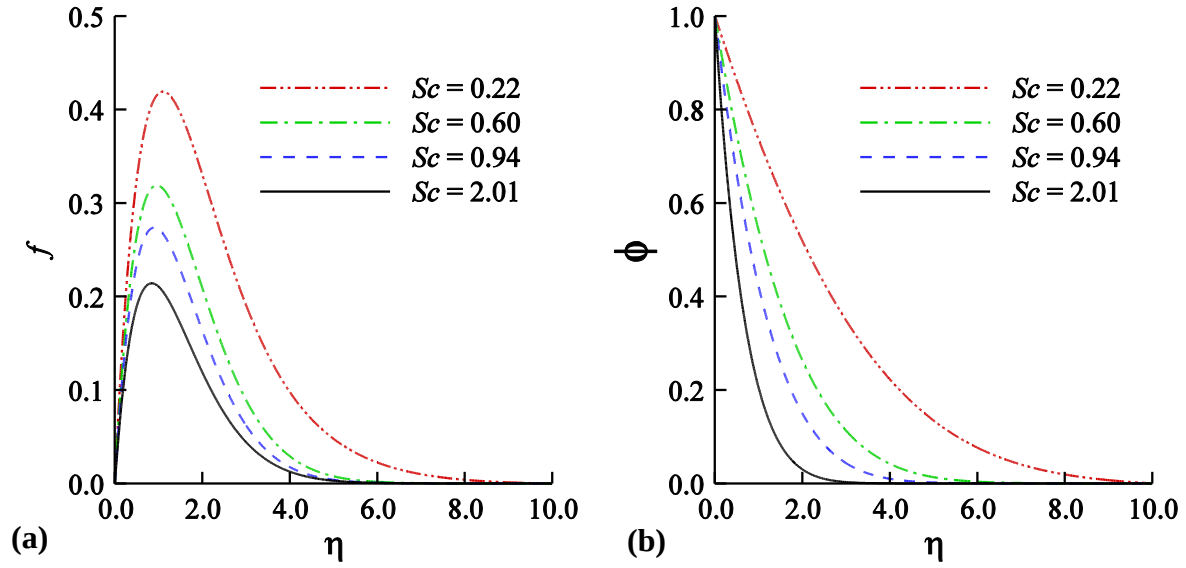

Figure 3. (a) Velocity and (b) concentration profiles at t = 1.0 for different values of *Sc* = 0.22, 0.60, 0.94, 2.01 while *Pr* = 0.7, λ = 1.0, and ω = 0.5.

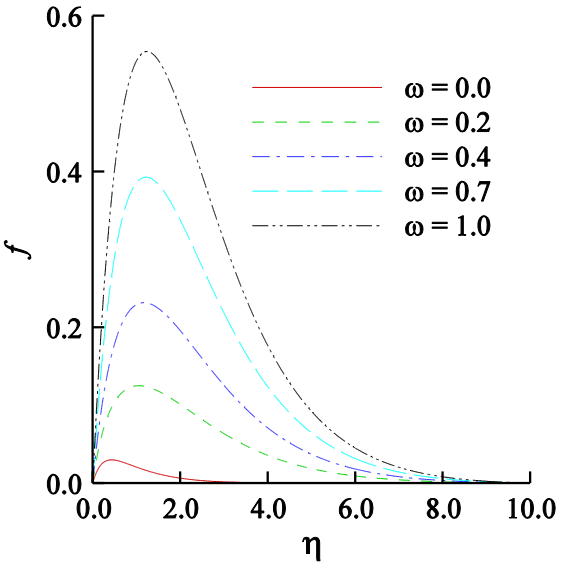

Figure 4. Effect of combined buoyancy parameter ω on the velocity profiles at t = 1.0 while Pr = 0.70, Sc = 0.22 and suction parameter λ = 0.5.

In many physical processes, it is important to control the boundary layer thickness. This can be achieved by a number of ways, however most of the times it is done by injection or suction of fluid, for this we have introduced a parameter λ. The effect of suction parameter on the temperature, concentration and velocity profiles is elaborated in Figure 5. Results suggest that the velocity, concentration and temperature profiles for Pr = 0.70, Sc =0.22, ω =0.5 at t =1.0 for different values of the suction parameter λ. The curve for λ = 0 i.e. when the fluid particles are not being sucked out. From the figure, we observe that the boundary layer thickness is maximum for this case. When the value of suction parameter λ is increased, it causes a decrease in the boundary layer thickness. Also, the velocity at a particular point decreases with the increase in suction parameter λ. When the value of λ is increased, it means that the fluid is being taken out more rapidly. Consequently, molecules will get less time to increase their temperature, hence we encounter smaller velocities. From Eqs. (52)-(54) and Eqs. (69)-(71), we come to know that for $\lambda \to 0$, we cannot get analytical solution. However, we can determine solutions numerically even for λ = 0.

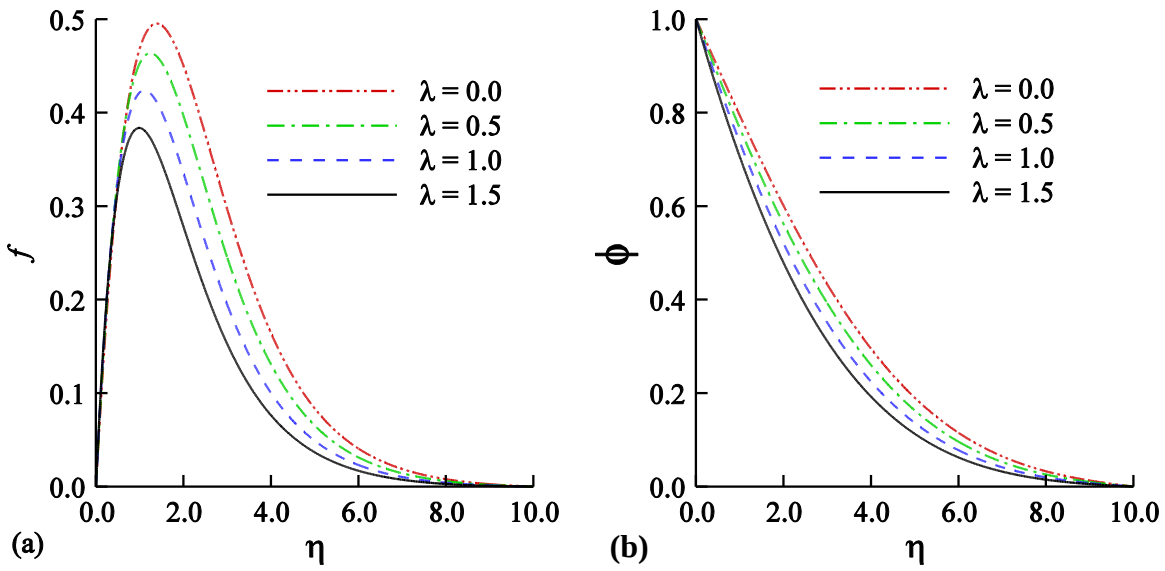

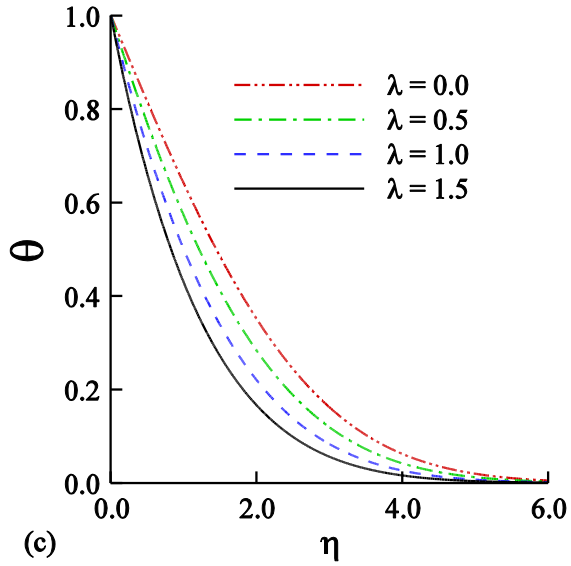

Figure 5. (a) Velocity, (b) concentration and (c) temperature profiles for different values of suction parameter λ at t = 1.0 while Pr = 0.70, Sc = 0.22 and ω = 0.5.

4.2 For water (Pr = 7.0)

Now we consider water (Pr = 7.0) as a fluid. The values of Sc for the different species that can be found in water are taken from Gebhart and Pera [16]. The effects of the Schmidt number Sc on the rate of mass transfer and shear stress are illustrated in Figure 6(a)-(b). From the figure it is evident that the rate of mass transfer is significantly affected by the values of Sc whereas there is rather weak influence on the shear stress. This is due to the fact that the mass diffusion of the fluid drastically decreases with increasing values of Sc; thereby the concentration gradient at the wall becomes high. In another way, for higher values of Sc small effect will be transported by the molecules, giving rise to larger values of concentration differences that result in increase of mass transfer. However, the kinematic viscosity of the fluid is higher for larger values Sc. For this reason, higher values of Sc reduce the shear stress.

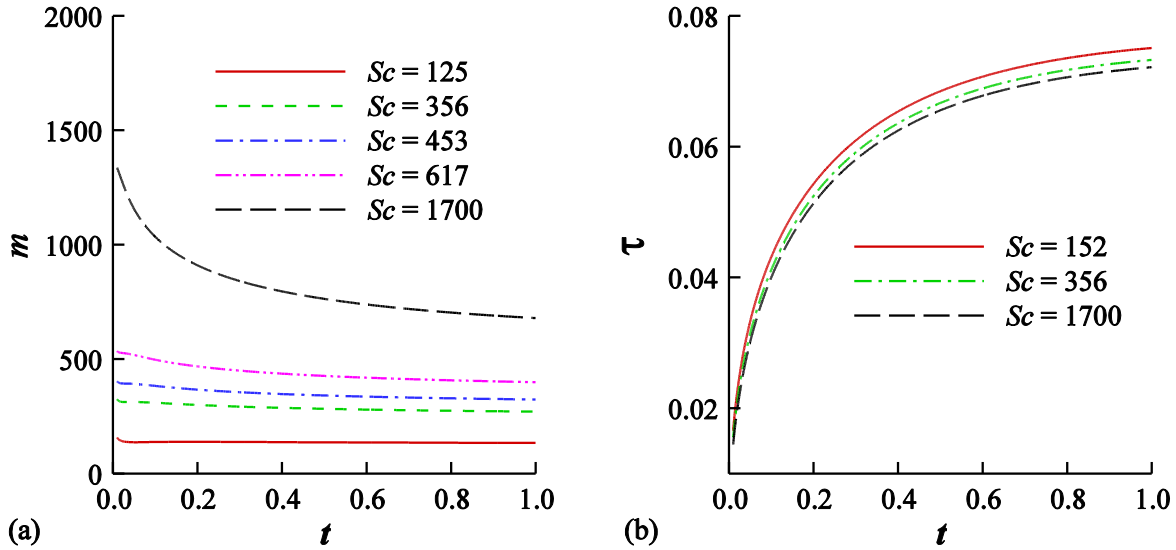

Figure 6. Numerical values of the (a) rate of mass transfer and (b) shear stress on the wall for water in presence hydrogen, oxygen, carbon dioxide, chlorine and sucrose for which Sc = 152, 356, 453, 617 and 1700, respectively.

Figure 7 shows the numerical results for velocity profiles of molecules in water at t = 0.5 in presence of different foreign species. The maximum value of the velocity is observed for Sc = 10.0, then velocities start decreasing as we increase the value of Sc owing to the fact that mass diffusivity of fluid decreases with increasing Sc.

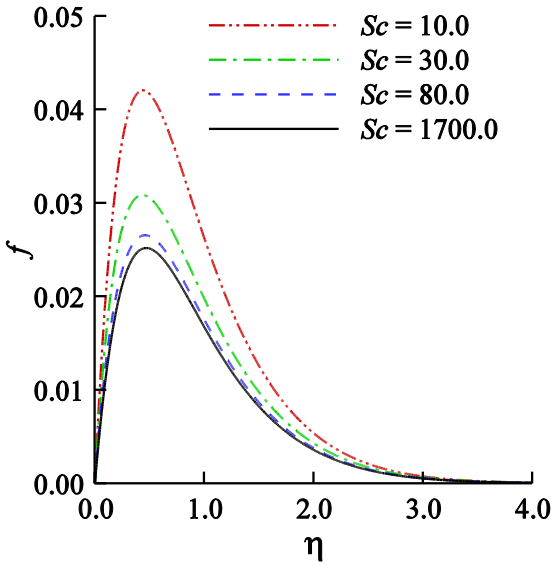

Figure 7. Velocity profiles for different values of Sc at t = 1.0 while Pr = 7.0, λ = 1.0 and ω = 0.5.

The variations of the velocity profiles and the rate of shear stress with the change of the combined buoyancy parameter ω are depicted in Figure 8(a)-(b), respectively. The value of ω measures the contribution of temperature and concentration differences in causing the buoyancy forces. When ω = 0, the density gradients are only caused only by the thermal differences. In this case, we are encountering maximum velocities. The velocity profiles in Figure 8(a) are computed at t = 1.0 for Pr = 7.0 in presence of H_2 (Sc = 152). The curve relating to ω = 0.5 is showing the velocities of the fluid particle when there is equal contribution of concentration differences and temperature differences in driving the flow. If we consider the flow due to concentration differences only (for which ω = 1.0), then the observed velocities are small to extent that the curve lies on the η-axis. In Figure 8(b), the numerical values of shear stress on the wall for different ω are presented. The values of shear stress are also found to decrease with increasing values of ω. It is attributed to the decrease in velocities for higher values of ω. The smallest value of shear stress is encountered for ω = 1.0 i.e. concentration differences solely causing buoyancy effects.

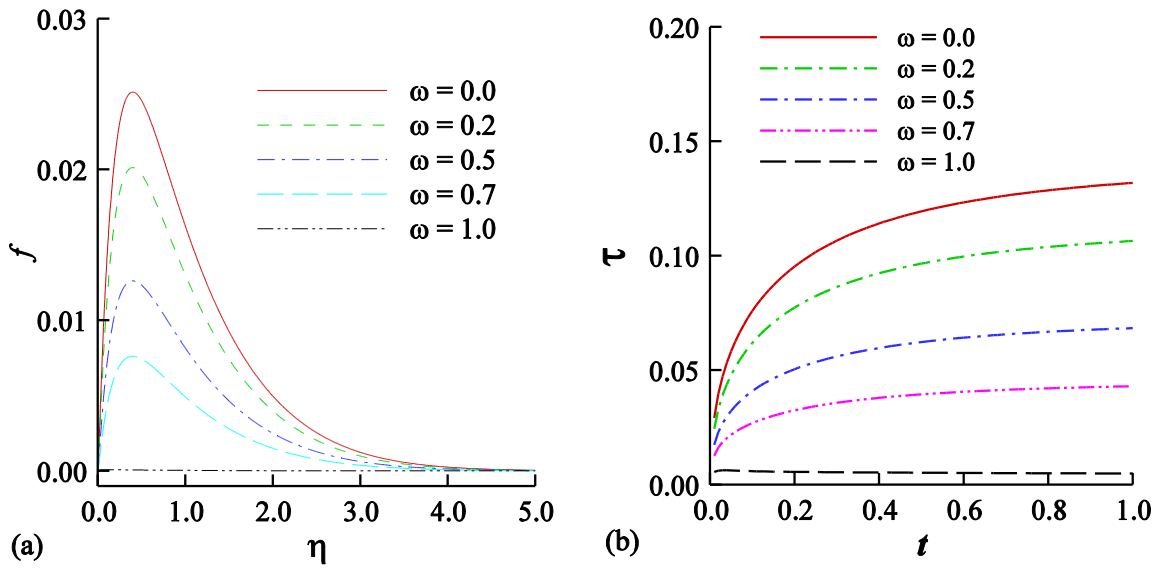

Figure 8. (a) Velocity profiles at t = 1.0 and (b) shear stress for different values of combined buoyancy parameter ω where Pr = 7.0, Sc = 152 and suction parameter λ = 1.0.

The influences of the suction parameter λ on the velocity, concentration and temperature profiles are demonstrated in Figure 9(a)-(c), respectively. It is noted that the effect of suction parameter is important due to the fact that it is used to control boundary layer thickness in many control processes. It is observed that the thicknesses of momentum, thermal and concentration boundary layers decrease owing to the increase of λ. If we look upon the boundary layers, it is worthy of mentioning that the concentration boundary layer thickness is the smallest of all others, that is justified, since Sc > Pr. The momentum boundary layer thickness is greater than the concentration and thermal boundary layer thickness because the values of Pr and Sc both are higher than unity, i.e. $\nu > \alpha$, $\nu > D$.

5. Conclusions

In this study, we examined how the thermal and molecular diffusion affect the transient free convection flow along an infinite vertical porous plate. The governing equations are transformed into a system of equations valid for short, long and all time. We utilized Keller Box method to determine the solutions for all time, however, the equations for short and long time were solved analytically. We made a comparison between the numerical solutions for all time and the analytical solutions for short and long time, which demonstrated a good agreement. In the case of air, it is observed from the results that the increasing values of Sc significantly reduces the momentum and concentration boundary layers. However, the maximum velocity increases due to the increase of the combined buoyancy parameter. In the case of water, the maximum velocity and the shear stress were found to decrease for higher values of the combined buoyancy parameter. But, the momentum, thermal and concentration boundary layers decreased with the increase of the suction parameter irrespective of the fluid.

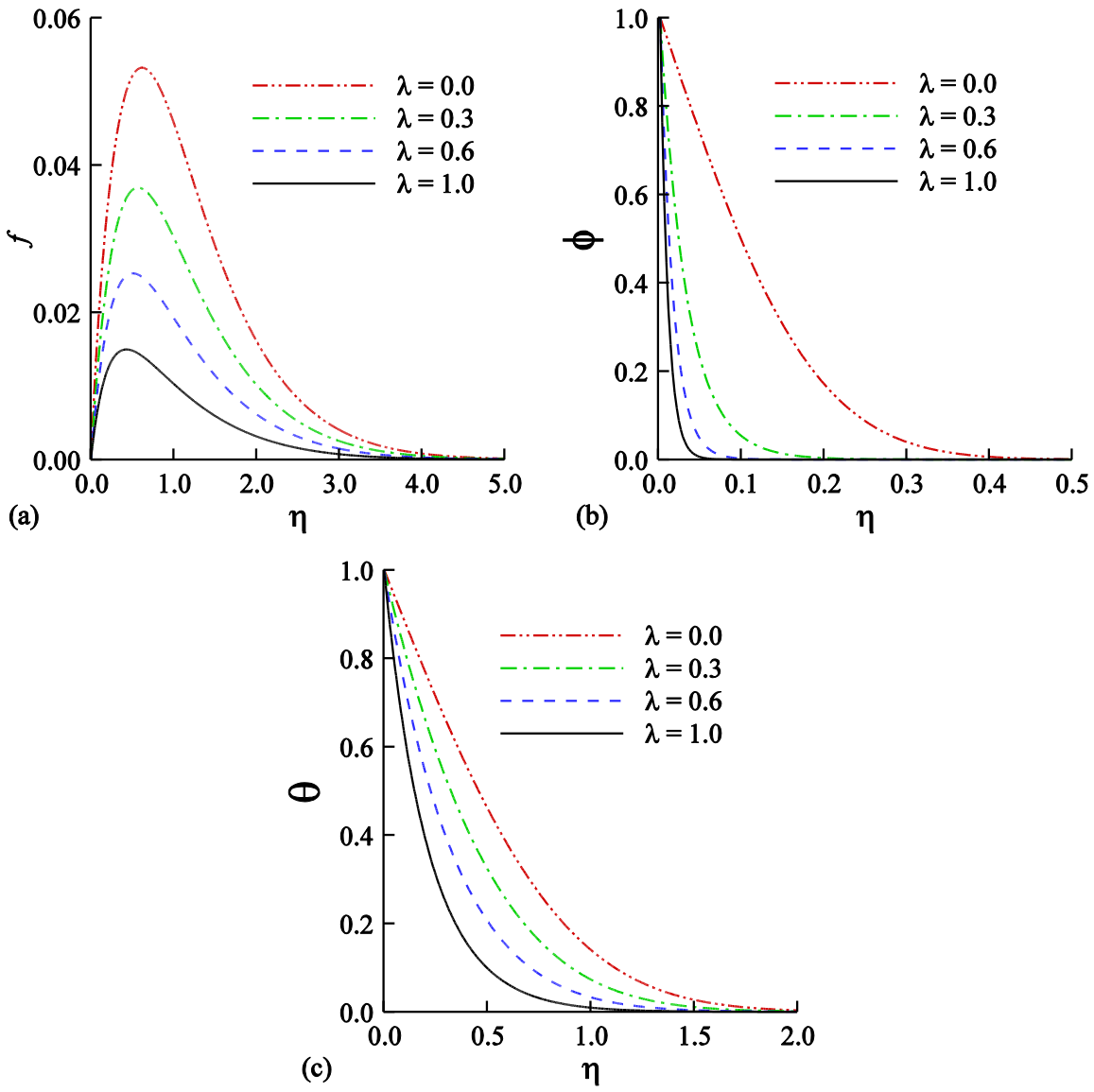

Figure 9. (a) Velocity (b) concentration and (c) temperature profiles at t = 1.0 for different values of suction parameter λ while Pr = 7.0, Sc = 152 and ω = 0.5.

References

[1] T. S. Chen and C. F. Yuh, Combined heat and mass transfer in natural convection on inclined surfaces, Num. Heat Transf., vol 2(2), pp. 233-250, 1979.

[2] E. V. Somers, Theoretical consideration of combined thermal and mass transfer from a vertical flat plate, J. Appl. Mech., vol 23, pp. 295-301, 1956.

[3] W. R. Wilcox, Simultaneous heat and mass transfer in free convection, Chem. Eng. Sci., vol 13, pp. 113-119, 1961.

[4] W. N. Gill, E. Deleasal and D. W. Zec, Binary diffusion and heat transfer in laminar free convection boundary layer on vertical plate, Int. J. Heat Mass Transf., vol 8, pp. 1131-1151, 1965.

[5] B. Gebhart, and L. Pera, The nature of vertical natural convection flow from the combined buoyancy effects on thermal and mass diffusion, Int. J. Heat Mass Transfer, vol 14 (12), pp. 2024-2050, 1971.

[6] L. Pera and B. Gebhart, Natural convection flows adjacent to horizontal surface resulting from the combined buoyancy effects of thermal and mass diffusion, Int. J. Heat Mass Transf., vol 15, pp. 269-278, 1972.

[7] M. A. Hossain, Simultaneous heat and mass transfer on oscillatory free convection boundary layer flow, Int. J. Energy Research, vol 12, pp. 205-216, 1988.

[8] M. A. Hossain and R. A. Begum, Effects of mass transfer on the unsteady free convection flow past an accelerated vertical porous plate with variable suction, Astrophys. Space Sci., vol 115, pp. 145-154, 1985.

[9] M. A. Hossain and A. C. Mandal, Mass transfer effects on the unsteady hydromagnetic free convection flow past an accelerated vertical porous plate, J. Phys., vol 18, pp. L63-L69, 1985.

[10] I. Pop, D. B. Ingham, Convective Heat Transfer, 1st ed., Pergamon, 2001.

[11] J. P. Holman, Heat Transfer, McGraw-Hill, New York, 1972.

[12] H. Schilichting and K. Gersten, Boundary-Layer Theory, 9th ed., Springer, 2017.

[13] H. B. Keller and T. Cebecci, Accurate numerical methods for boundary-layer flows. Part-I, Two dimensional laminar flows, Proceedings of the International conference on Numerical Methods in Fluid Dynamics, Lecture notes in Physics, Springer, 1971.